Measurement of Photonic Mode Dispersion and Linewidths in Silicon-on-Insulator Photonic Crystal Slabs

M. Galli, D. Bajoni, M. Belotti, F. Paleari, M. Patrini, G. Guizzetti, D. Gerace, M. Agio, L. C. Andreani, D. Peyrade, and Y. Chen

***Abstract*—The dispersion of photonic modes in one-dimensional (1-D) and two-dimensional (2-D) patterned silicon-on-insulator (SOI) waveguides, also containing line defects, is fully investigated both above and below the light line. Quasi-guided (radiative), as well as truly guided modes are probed by means of angle- and polarization-resolved microreflectance and attenuated total reflectance measurements. For the 1-D case, the sharp resonances observed in reflectance spectra are analyzed in terms of the Airy-Fano model, and the measured linewidths are shown to be very close to theoretical predictions. In the 2-D lattices containing W1 line defects the presence of a supercell repetition leads to the simultaneous excitation of defect and bulk modes which are folded in a reduced Brillouin zone. The measured dispersion is in very good agreement with full three-dimensional calculations based on expansion on the waveguide modes, indicating that a deep understanding of the propagation properties of patterned SOI waveguides is achieved.**

***Index Terms*—Dispersion, optical spectroscopy, photonic crystals (PhCs), waveguides.**

I. Introduction

PERIODICALLY patterned planar waveguides are emerging as one of the best performing structures for the control of light propagation in three dimensions (3-D) [1]–[4]. This is obtained by means of a two-dimensional (2-D) photonic lattice embedded in a slab waveguide, which provides additional confinement in the vertical direction by means of total internal reflection. These structures support two kinds of modes; quasi-guided (leaky) and truly guided. The former modes can couple to external radiation and posses an intrinsic linewidth related to out-of-plane radiation losses, while the latter modes are Bloch states whose energy lie below the light line of the cladding material and propagate with very low losses. In this respect, truly-guided modes are more suitable for microphotonic applications.

The existence of truly guided modes in photonic crystal (PhC) slabs requires a high dielectric contrast between core and cladding materials. For this reason, silicon-on-insulator (SOI) patterned waveguides has become one of the preferred systems for the study and design of micro-optical devices, as well as for the very well developed silicon technology.

The experimental determination of photonic band dispersion both above and below the light line is extremely important for fundamental research, as well as for applications, as it contains full information on the propagation properties of these systems. In the following, we show that a deep understanding of photonic mode dispersion over the whole reciprocal space can be obtained by optical spectroscopy means, especially by attenuated total reflectance (ATR), which is applied here for the first time to these systems.

II. Sample Fabrication

One- and two-dimensional PhC structures were patterned in commercial silicon-on-insulator wafers (SOITEC) by means of electron beam lithography (EBL) followed by reactive ion etching (RIE). The waveguides consisted in a 260-nm-thick Silicon core on a 1-μm-thick SiO_2 cladding grown on a silicon substrate. EBL was performed on PMMA resist using a JEOL JBX5D2U vector scan generator at 50 keV energy. After developing the PMMA, pattern transfer to the waveguide core was realized through a liftoff process for 1-D samples, and a three-layer process for 2-D samples, respectively. In the liftoff procedure, a thin nickel layer is evaporated onto the silicon surface and lifted off by dissolution of the PMMA. RIE is then performed in a Nextral NE110 system by means of a SF6/CHF3 gas mixture at a pressure of 10 mT and a radio frequency (rf) power of 15 W. The etching rate is typically 50 nm/min and RIE parameters are optimized for steeper sidewalls. Finally, the remaining Ni mask is removed in a nitric acid solution. For the three-layer process, the system consisted of a 500-nm-thick S18 optical resist bottom layer, a 50-nm-thick Ge middle layer and a 150-nm-thick PMMA top layer. The top and middle layers

Manuscript received October 2, 2004. This work was supported in part by the Cofin 2002 Program "Silicon-based photonic crystals: Technology, optical properties and theory" and in part by the FIRB Project "Miniaturized electron and photon systems."

M. Galli, D. Bajoni, F. Paleari, M. Patrini, G. Guizzetti, D. Gerace, M. Agio, and L. C. Andreani are with the INFM and Dipartimento di Fisica "A. Volta," Università degli Studi di Pavia, Pavia I-27100, Italy (e-mail: galli@fisica volta.unipv.it; bajoni@fisicavolta.unipv.i; paleari@fisicavolta.unipv.it; patrini @fisicavolta.unipv.it; guizzetti@fisicavolta.unipv.it; gerace@fisicavolta.unipv. it; agio@fisicavolta.unipv.it; andreani@fisicavolta.unipv.it).

M. Belotti is with the INFM and the Dipartimento di Fisica "A. Volta," Università degli Studi di Pavia, Pavia I-27100, Italy, and also with the Laboratoire de Photonique et de Nanostructures, LPN-CNRS, Marcoussis F-91460, France (e-mail: belotti@fisicavolta.unipv.it).

D. Peyrade was with the Laboratoire de Photonique et de Nanostructures, LPN-CNRS, Marcoussis F-91460, France. He is now with CNRS-LTM, CEA-LETI, 38054 Grenoble Cedex 9, France (e-mail: david.peyrade@cea.fr).

Y. Chen is with the Laboratoire de Photonique et de Nanostructures, LPN-CNRS, Marcoussis F-91460, France, and also with the Département de Chemie, Ecole Normale Supérieure, Paris 75231, France (e-mail: yong.chen@lpn.cnrs.fr; yong.chen@ens.fr).

Digital Object Identifier 10.1109/JSAC.2005.851164

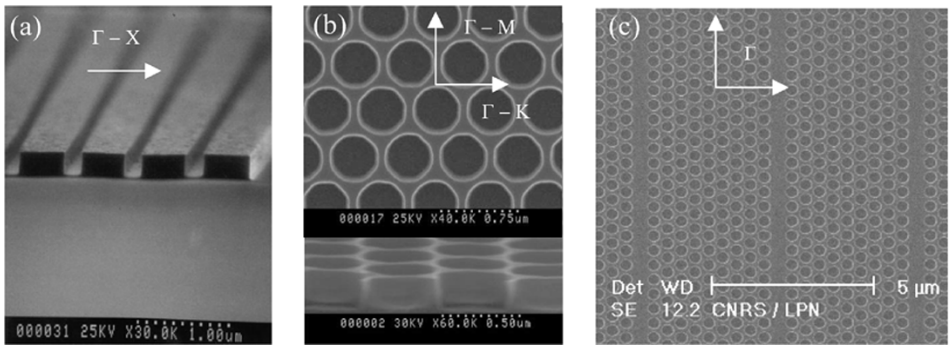

Fig. 1. Scanning electron micrographs of SOI PhC slabs. (a) 1-D array of air stripes. (b) 2-D triangular lattice of air holes. (c) 2-D triangular lattice of air holes containing W1 line defects repeated with supercell periodicity $d = 5\sqrt{3}a$.

were etched by standard RIE techniques, while the silicon top layer is etched by RIE using a SF_6 and CHF_3 gas mixture. Also, in this case, the RIE parameters were optimized to obtain vertical sidewalls in silicon [5].

Several different samples were fabricated in this way: 1) a 1-D array of air stripes with lattice constant $a = 650$ nm and 0.18 air fraction; 2) a 2-D triangular array of air holes with lattice constant $a = 500$ nm and hole radius $r = 0.34a$; and 3) a 2-D triangular array of air holes with lattice constant $a = 500$ nm and hole radius $r = 0.34a$ containing W1 defects (a missing lines of holes along the Γ-K direction). In this latter case, W1 defects were repeated with different supercell periodicities $d = m\sqrt{3}\,a(m = 4, 5, 6)$ along the Γ-M direction. Scanning electron micrographs of the samples are shown in Fig. 1.

III. Optical Characterization

The optical response in the radiative region, i.e., above the light line, has been probed by means of angle-resolved specular reflectance from the sample surface. This technique has been applied before to measure the band dispersion of 1-D and 2-D PCs [6]–[8]. It relies on the observation of resonant structures in the polarized reflectance spectra that exhibit a well-defined dispersion as a function of the angle of incidence. These can be ascribed to excitation of photonic modes of the system, which occurs whenever the energy and the wavevector of the incoming beam match those of an allowed propagating mode. By varying the angle of incidence and energy of the light, the photonic band dispersion of the sample can be experimentally determined in a large part of the Brillouin zone. The major drawback of this technique is that only radiative modes, which lie above the light line, can be excited, while it is not suitable to probe the dispersion of the truly guided modes, which extend in the cladding regions and are evanescent in air. This limitation can be overcome by means of angle-resolved ATR. By placing a high-index prism at a small distance from the surface of the sample, efficient coupling between the evanescent fields at the air-prism-sample interfaces can be achieved, therefore allowing the excitation of truly guided modes that lie below the light line. This way, the energy-wavevector range accessible in the experiment is greatly enhanced, and detailed information on the dispersion of guided photonic modes can be obtained up to the edge of Brillouin zone. The experimental configuration for ATR measurements is shown in Fig. 2: a ZnSe hemisphere, acting as a prism with

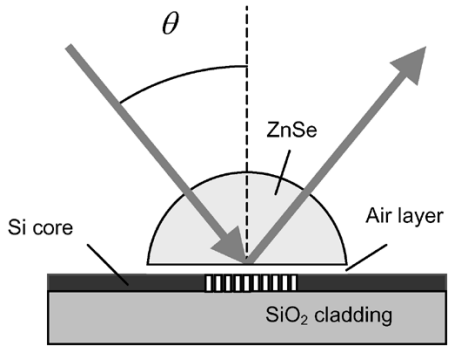

Fig. 2. Experimental configuration for the measurement of attenuated total reflectance.

refractive index $n = 2.4$, is kept close to the sample surface leaving a very thin air layer in between. The thickness of the air layer, which determines the coupling strength between evanescent fields at the sample-prism interface, is found to be a critical parameter in the experiment. For this reason, the ZnSe prism is mounted on three piezoelectric actuators which allow a fine control of the separation and alignment with the sample surface.

Angle-resolved specular reflectance and ATR from the sample surface are measured in the spectral range 0.3–1.8 eV, at a spectral resolution of 0.5 meV, by means of a microreflectometer coupled to a Fourier-transform spectrometer (Bruker IFS66s). The angle of incidence θ is varied in the range of 4°–75° with an angular resolution of 0.5° set by the very small but finite-numerical aperture of the beam that is focused on the sample. Transverse-electric (TE) and transverse-magnetic (TM) polarizations with respect to the plane of incidence are selected by means of KRS5 wire-grid and calcite Glann–Taylor polarizers.

IV. Theoretical Treatment

In order to calculate the photonic band dispersion of the patterned waveguides, a method has been used [9] in which the magnetic field is expanded onto the basis consisting of the guided modes of a homogeneous air/Si/SiO_2 waveguide, and the core layer is taken to have an average, uniform dielectric constant. The second-order equation for the magnetic field is transformed into a linear eigenvalue problem, which is solved by numerical diagonalization, like in usual plane-wave calculations. The guided modes of the effective homogeneous

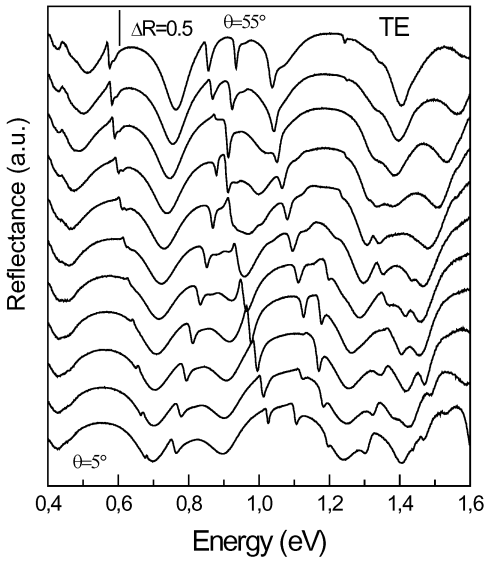

Fig. 3. Reflectance measurements along the Γ-X orientation for TE polarization on the 1-D sample. The curves are vertically shifted for clarity. Only a selection of curves from 5° to 55° with step of 5° are shown.

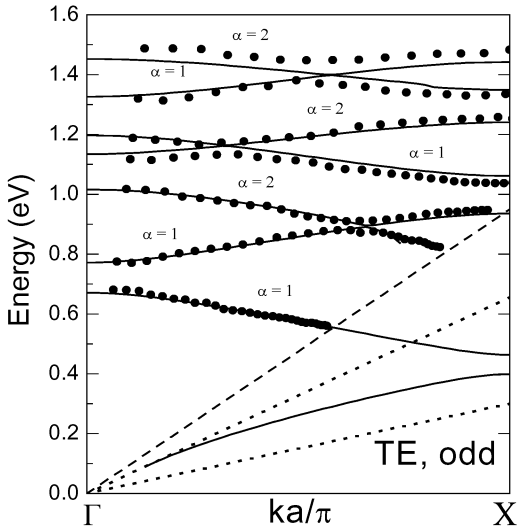

Fig. 4. Measured dispersion (full circles) compared with calculated bands (solid lines) for the 1-D sample. The index α indicate the order of photonic modes, while the light lines of air (Si and SiO_2) are represented by dashed (dotted) lines.

waveguide are folded in the first Brillouin zone and are coupled by the off-diagonal components of the inverse dielectric tensor, leading to band splittings. This approach yields the energy dispersion of the guided modes whose energies lie below the light lines of the upper and lower claddings, as well as of the modes that lie above the two light lines when folded in the first Brillouin zone. Coupling of the latter states to the leaky modes of the waveguide is taken into account by first-order perturbation theory [10], [11] and yields the imaginary part of the energy that corresponds to intrinsic radiation losses, i.e., out-of-plane diffraction. The spectral linewidths of resonant structures in reflectance spectra are given by twice the imaginary part of the corresponding photonic mode.

As a complementary approach, we calculate the reflectance and transmittance spectra of the layered system by the well-known scattering-matrix method [12]. This numerical method is an exact solution of Maxwell equations and it contains all radiative effects in the structure. In the present case, we have four layers: air, patterned silicon, unpatterned SiO_2, and Si substrate. The frequency-dependent complex dielectric constants of Si and SiO_2 are used in the calculation. The extension to ATR spectra is performed by taking the incoming beam in the prism material and introducing an additional air layer between the prism and the patterned silicon layer.

V. Results and Discussion

A. 1-D Array of Air Stripes

The angle-resolved reflectance spectra of the sample with 1-D array of air stripes are shown in Fig. 3, for TE polarized light incident along the Γ-X orientation. The angle of incidence is varied from 5° to 65° with steps of 2.5°, and the spectra are shifted vertically (each one by the same quantity) in order to facilitate viewing. Only a selection of spectra is shown in Fig. 3. Fig. 4 shows the corresponding photonic bands as extracted from experimental data and compared with calculated bands for this structure. A detailed discussion of the spectra and photonic bands for the same sample has already been published [13]. In the following, we recall the main features of this system, and then turn to the analysis of the spectral resonances appearing in reflectance curves.

As it is immediately evident from Fig. 4, there is a fairly good agreement between measured dispersion and calculated bands. Even though small discrepancies arise for bands at high energy, all the peculiar characteristics of the band diagram such as energy gaps and band crossings are well reproduced by experiments. A second-order waveguide mode appears for energies above 0.8 eV (the order of guided modes is indicated on each curve by the index α).

By looking at the band diagram reported in Fig. 4 we notice that guided modes, i.e., modes whose dispersion is confined between the Si core and the SiO_2 dispersion lines, are present for TE polarization. Moreover, we notice that the lowest band in the guided mode region has a finite cutoff wavelength imposed by the thickness of the asymmetric waveguide. The guided modes go over smoothly into the radiative region when crossing the light line and are thereafter viewed as resonances or quasi-guided modes in reflectance spectra, as appears in experiments. Due to radiation losses, such quasi-guided modes have a finite lifetime, which means that resonances observed in reflectance spectra are expected to exhibit an intrinsic linewidth. For a sample where broadening effects due to disorder or imperfections may be neglected, it is therefore of great interest to study the evolution of the intrinsic linewidths in the energy-wavevector space, since they are directly related to radiation losses suffered by the photonic modes during propagation along the waveguide. This can be done by evaluating the full-width-half-maxima (FWHM) of the narrow resonances observed in the experimental spectra. However, by looking at the measured resonances, we notice that they may assume very different shapes (i.e., maxima, minima, or even a dispersive-like shape) depending on their position relative to the interference background, which is always present in the spectra due to the

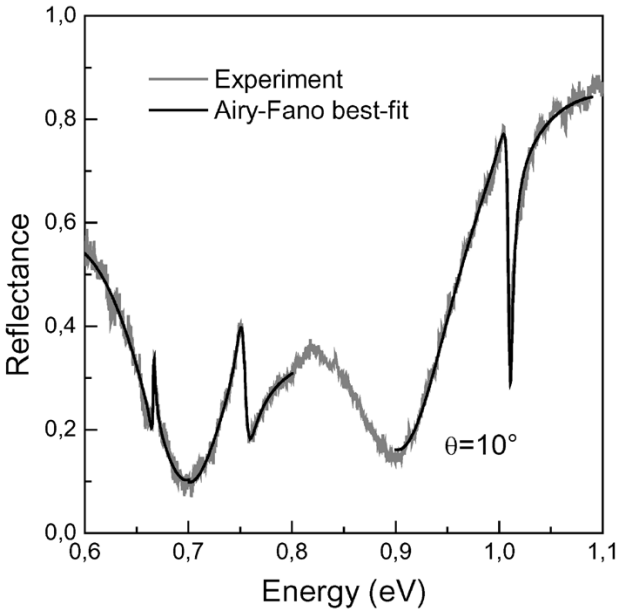

Fig. 5. Best fit according to the Airy–Fano model for the first three resonances observed in the 10° reflectance spectrum of the 1-D sample. Notice the high quality of the fit regardless of the resonance shape (i.e., maxima, minima, or dispersive-like).

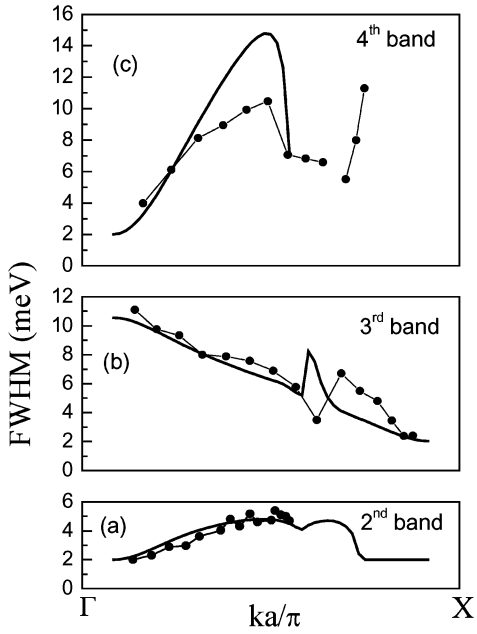

Fig. 6. Measured (full circles) and calculated (gray lines) FWHM for the second, third, and fourth band of Fig. 3. An instrumental broadening of 2 meV has been added to the calculated linewidths in order to account for the small spread in the wavevector caused by the small numerical aperture of the light beam incident on the sample.

multilayer structure of the SOI waveguide. For this reason, a best fit procedure should be applied to each resonance in order to extract an appropriate FWHM without ambiguity. In our case, we adopted the Airy–Fano model [8], [14], where the reflectivity $R(\omega)$ of the sample is expressed by

$$R(\omega) = A(\omega) + F(\omega).$$

Here, $A(\omega)$ is the Airy function, which describes the background interference pattern, while $F(\omega)$ is the Fano term

$$F(\omega) = F_0 \frac{\left[q + \frac{2(\omega-\omega_0)}{\Gamma}\right]^2}{1 + \left[\frac{2(\omega-\omega_0)}{\Gamma}\right]^2}$$

where ω_0 is the frequency of the resonance, Γ is the FWMH, and F_0 an oscillator strength. The factor q may assume values between -1 and $+1$ and determines the shape of the resonance. Very good fits to experimental data are obtained by means of this model, as shown in Fig. 5 for the lowest energy resonances corresponding to the second, third, and fourth photonic bands in Fig. 4. By applying this fitting procedure to reflectance spectra for each angle of incidence, we trace the evolution of the linewidths in the k-space. This is shown in Fig. 6, where the measured linewidths are compared with FWMH calculated as twice the imaginary part of the photonic mode's energy. There is an overall good agreement between measured and calculated FWMH.

The only noticeable discrepancy is observed at $ka/\pi = 0.6$ in Fig. 6(b), where the experimental FWHM goes in the opposite direction as compared with the theoretical prediction. This is probably due to crossing of bands 3 and 4 around 0.9 eV and to the strong mixing in the crossing region, which makes it very difficult to separate contributions from the third and fourth bands in the measurement. Notice that a small (2 meV) instrumental broadening has been added to the calculated linewidths in order to account for the small spread in the wavevector of the incident light caused by the small numerical aperture of the measuring beam. At the Γ point, bands 2 and 4 are theoretically lossless, while only band 3 has a finite-imaginary part of the frequency. This indicates that besides the truly guided modes, also some radiative modes could be of interest for applications requiring relatively low losses, as previously noticed [15], [16]. A complete theoretical analysis of radiative losses in 1-D PhC slabs is presented elsewhere [17].

B. 2-D Triangular Lattice of Air Holes

Angle-resolved reflectance spectra for the 2-D l bulk sample (without linear defects) were measured along both symmetry orientations and for both polarizations. Results obtained along the Γ-K orientation for TE and TM polarizations are shown in Fig. 7(a) and (b), respectively. Angle- and polarization-resolved spectra were also measured for light incident along the Γ-M orientation (not shown). Similarly to what observed for the 1-D sample, the curves display a prominent interference pattern due the multiple interference occurring at the core-cladding and cladding-substrate interfaces. Superimposed to the interference fringes, several sharp features that mark the excitation of photonic modes are clearly visible in the spectra. A comparison between measured and calculated photonic bands is shown in Fig. 8. Notice that an incident field with TE (TM) polarization is odd (even) with respect to the plane of incidence. The photonic modes in Fig. 8 are also classified according to mirror symmetry with respect to the plane of incidence, which is a good symmetry operation along the directions Γ-M, Γ-K, and which we call σ_{kz}. Therefore, modes which are excited by TE-polarized light are compared to photonic bands having symmetry $\sigma_{kz} = -1$, and modes which are excited by TM-polarized light are compared with bands having symmetry $\sigma_{kz} = +1$. We notice also

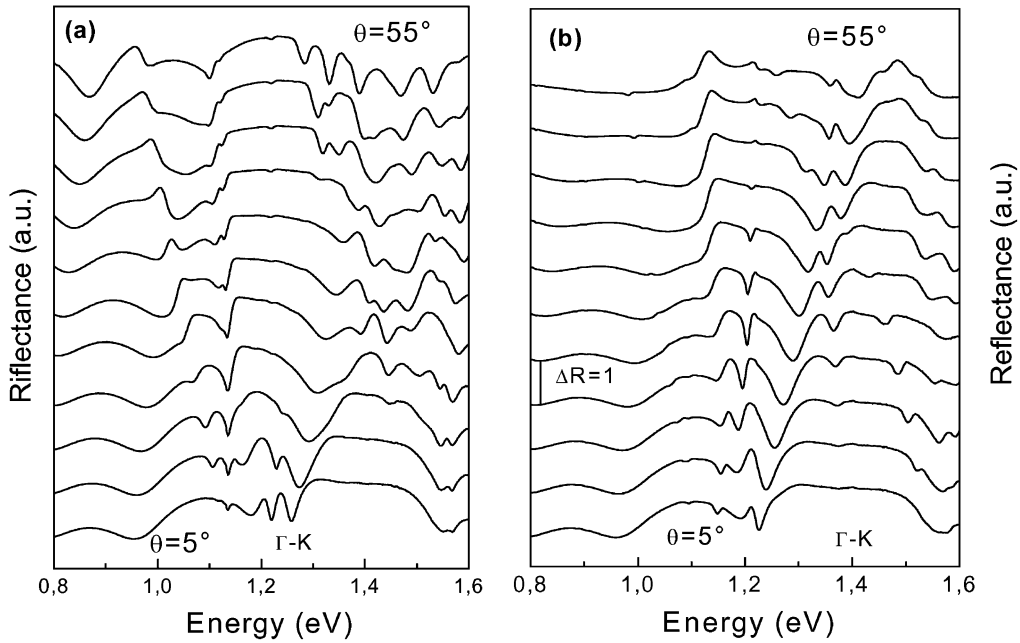

Fig. 7. Reflectance spectra measured along the Γ-K orientation for (a) TE and (b) TM polarizations on the 2-D sample. Measurements are performed from 5° to 55° with step of 5° and the curves are vertically shifted for clarity.

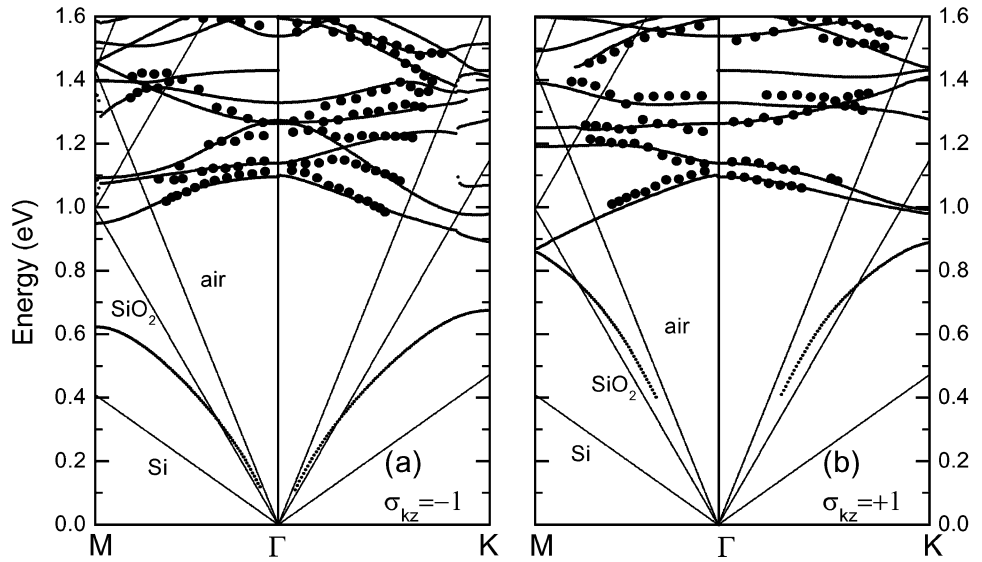

Fig. 8. Measured dispersion (full circles) compared with calculated bands of the 2-D sample for (a) TE and (b) TM polarizations. Light lines of air, Si, and SiO_2 are represented by thin dotted lines.

that some modes change parity on changing the symmetry direction of the Brillouin zone. This is evident for the photonic mode around 1.4 eV in Fig. 8, which changes from TE to TM on changing from the Γ-M to the Γ-M orientation, respectively. This apparent discontinuity in the band diagram can be understood by considering that the vertical mirror plane changes when turning from the Γ-K to the Γ-M orientation, i.e., TE and TM modes change parity with respect to the σ_{kz} operator, as already shown by measurements on macroporous Si PhCs [18].

Rather good agreement between theory and experiment is obtained for the dispersion and energy of photonic bands for both TE and TM polarizations. In particular, the dispersion of the lowest bands up to ∼1 eV is fairly well reproduced, whereas small discrepancies between experiment and calculations can be seen for higher energy bands. This may be attributed to the dispersion of the refractive index of the layers, which has not been included in calculations, and to effects of disorder that become more important on increasing the energy.

It is interesting to compare the bands of the PhC slab with those of an ideal 2-D structure. For a 2-D PhC, the photonic bands are usually classified according to mirror symmetry with respect to the 2-D plane, which we call σ_{xy}, and are often named H or TE modes ($\sigma_{xy} = +1$, electric field in the xy plane) and E or TM modes ($\sigma_{xy} = -1$, electric field along z). The SOI PhC slab is not symmetric with respect to an horizontal midplane, thus, its photonic modes cannot be rigorously classified according to the operator σ_{xy} [19]. In order to facilitate the comparison, we have calculated the band dispersion of a PhC slab

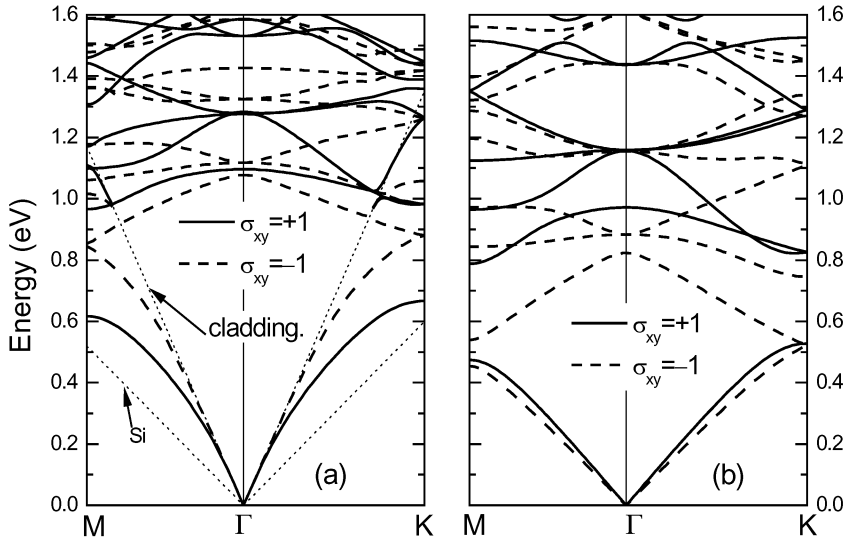

Fig. 9. Photonic bands calculated for (a) the PhC slab in the symmetric approximation and (b) for the ideal 2-D PhC. Bands are classified according to mirror symmetry with respect to the xy plane. Thin dotted lines in (a) are the light line of Si core and the average cladding material.

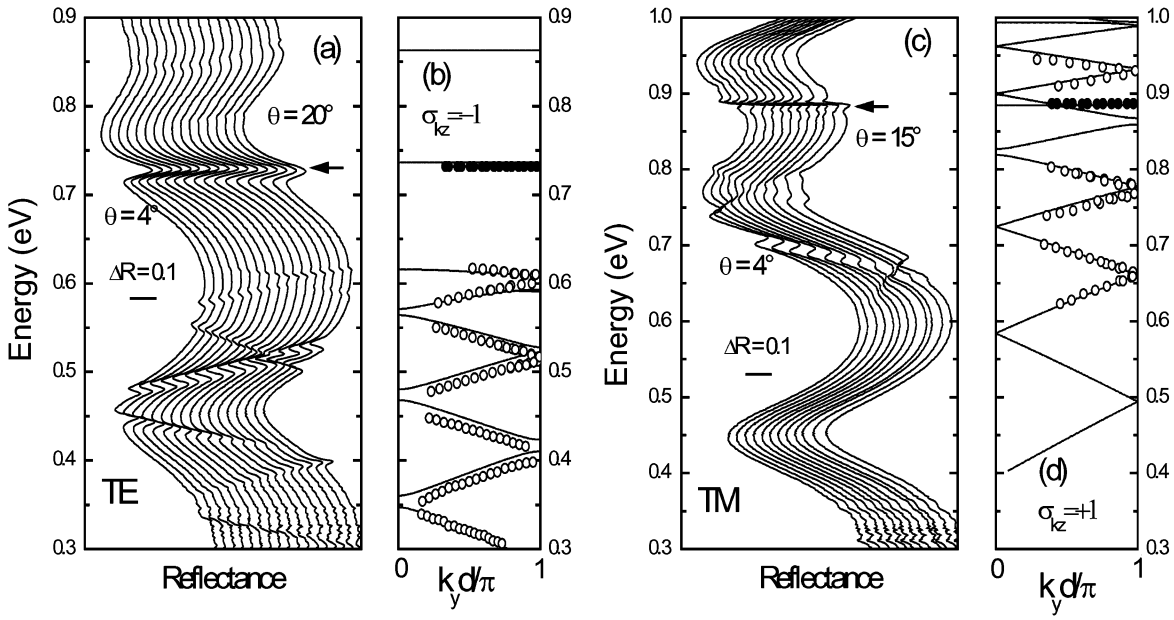

Fig. 10. (a) and (c) Reflectance measurements along the Γ-M orientation for TE and TM polarizations on the 2-D sample with W1 line defects. The spectra are taken at steps of 1° and are slightly shifted with respect to each other for clarity. (b) and (d) Corresponding photonic bands folded into a reduced Brillouin zone due to supercell periodicity. The defect modes at 0.73 and 0.89 eV for TE and TM polarizations, respectively, are indicated by arrows. (b) TE. (d) TM.

whose upper and lower claddings have the same dielectric constant $\varepsilon = 1.5$, which is the average between the values for air and SiO_2. These bands are shown in Fig. 9(a) being classified with respect to σ_{xy} (notice that $\sigma_{xy} = +1$ or -1 modes are sometimes referred to as TE-like or TM-like, respectively) and are seen to be almost identical to those of the SOI PhC slab shown in Fig. 8. The photonic bands of the ideal 2-D structure are then shown in Fig. 9(b) for comparison. It can be seen that the bands of the PhC slab differ from those of the ideal 2-D system in two respects: 1) the photonic bands of the PhC slab are blue-shifted due to vertical confinement in the slab and 2) the PhC slab becomes multimode above a cutoff energy of about 0.95 eV. From the point of view of polarization properties, it can be seen from Figs. 8 and 9 that an incident field with definite polarization with respect to the plane of incidence couples to both $\sigma_{xy} = +1$ and $\sigma_{xy} = -1$ modes. This effect, which is sometimes referred to as polarization mixing [6], indicates that the classification of the photonic modes according to symmetry σ_{kz} is the appropriate one when comparing with surface reflectance experiments, as already discussed [18].

C. 2-D Triangular Lattice of Air Holes With W1 Line Defects

Fig. 10(a) and (c) shows experimental reflectance spectra of sample W1 line defects shown in Fig. 1(c) measured along the Γ-M direction, i.e., orthogonal to the line defects, and for both polarizations. Also, in this case, resonant features corresponding to the excitation of photonic modes, which exhibit a marked dispersion with the incidence angle are clearly observed. Besides

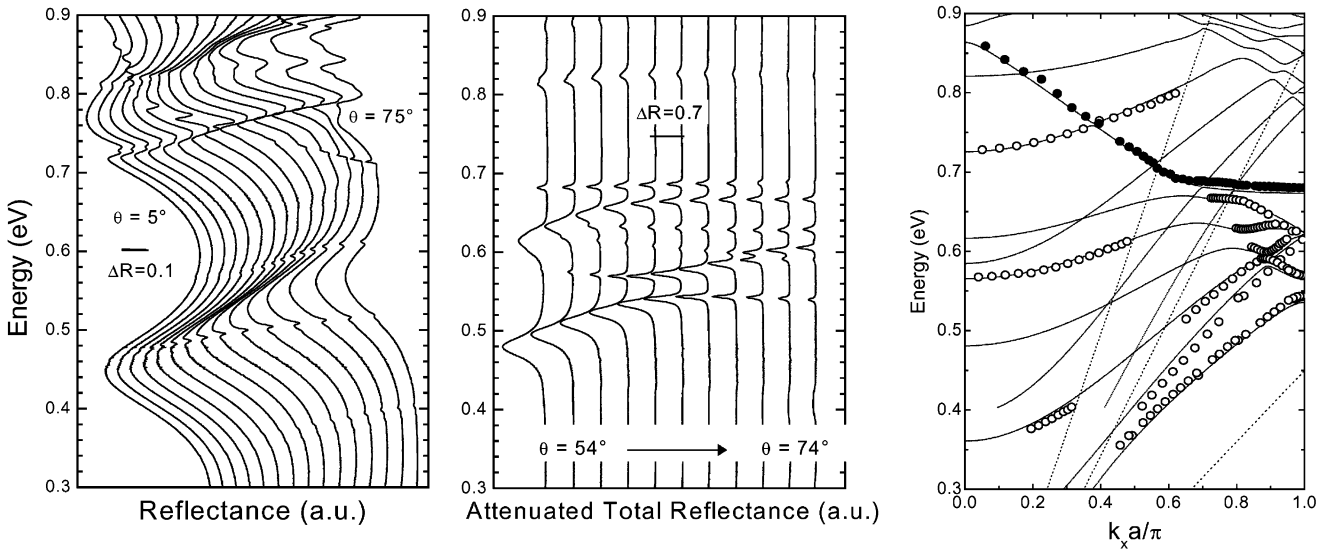

Fig. 11. (a) Experimental reflectance and (b) ATR spectra measured along the Γ-K orientation for TE polarizations on the sample with W1 line defects. (c) Measured (circles) and calculated band dispersion for TE or $\sigma_{kz} = -1$ (lines); the defect mode is indicated by full circles.

these, two dispersionless resonances occur at 0.73 and 0.89 eV for TE and TM polarizations, respectively. They correspond to the defect modes localized at the missing rows of holes, which act as cavities for propagation direction perpendicular to the line defect. A comparison with calculated dispersion is presented in Fig. 10(b) and 10(d). Excellent agreement is found between experimental and calculated bands. Notice that for this sample orientation the wave vectors of the modes are perpendicular to the line defects, and the photonic bands are folded into a reduced Brillouin zone due to the new, longer periodicity of the system. As a result, most of the bands fall above the light line and are observed in angle-resolved reflectance spectra.

The optical response of sample containing W1 line defects along the Γ-K direction were thoroughly studied by means of both angle resolved reflectance and ATR. The wavevectors of the photonic modes are in this case parallel to the line defects, which provides additional waveguiding of radiation along the defect: no localization of light is expected and the defect mode is, therefore, dispersive due to its finite group velocity, as observed from reflectance spectra shown in Fig. 11(a). Fig. 11(b) shows ATR spectra measured for the same sample orientation. In this case, excitation of guided modes appears as "absorption-like" dips on a flat, almost unitary background, which correspond to the total internal reflection regime. Notice that while resonances observed in reflectance spectra have amplitudes of the order of 0.05, those observed in ATR geometry can be deep as 0.8. This means that as much as the 80% of the incoming energy can be transferred to the PC slab by the prism-coupling. Such a highly efficient energy transfer is attributed to the overlap of the evanescent tails of the modes freely propagating in the ZnSe prism with those of the PC guided modes. This overlap mostly occurs in air spacer between the prism and the surface of the sample and the coupling is, thus highly dependent on their distance. When the prism is placed very close to sample surface, the modes are strongly affected by its presence and broad features appear in the spectra. The band dispersion is also affected and the energies of the features are slightly shifted. By increasing the width of the air spacer, the resonances become sharper and their energy positions stick with the values expected for the SOI PC slab. For the measurements in Fig. 11(b), the separation distance is ~ 250 nm, as obtained from a comparison with calculated ATR spectra (not shown here).

The combination of results obtained from normal reflectance and ATR spectra yields a very precise experimental reconstruction of the band dispersion of the sample, along the whole extent of the Brillouin zone. As a matter of fact, in the considered spectral range, the value of wavevectors obtained by means of the high-index prism are greater than π/a and the experimental points must, therefore, be reported in the first Brillouin zone by subtracting a reciprocal lattice vector. Excellent agreement is found between the experimental dispersion and the full 3-D calculations for TE polarization $(\sigma_{kz} = -1)$, as shown in Fig. 11(c). Analogous results are obtained for TM polarization and the dispersion of the TM $(\sigma_{kz} = +1)$ defect mode is found to be strongly different as compared with the TE defect mode [20].

Notice that the defect mode in Fig. 10(d) along the Γ-M orientation corresponds to the mode at $k = 0$ in Fig. 11(c) along the Γ-K orientation. The polarization character of the defect mode changes on turning from the Γ-M to the Γ-K orientation: this behavior corresponds to a change of the mirror plane of the PhC structure, like for the case of the triangular lattice previously discussed. Analogously, the defect mode around 0.73 eV in Fig. 10(b) corresponds to a defect mode measured in TM polarization along Γ-K (not shown here).

The dispersive behavior of the defect modes is traced in the reciprocal space from the low-k region across the light line up to the edge of the Brillouin zone. We emphasize that the combination of standard and attenuated total reflectance allows measuring the frequency-wavevector dispersion in a direct way, as both quantities are fixed by the experimental configuration. We observe that the $\sigma_{kz} = -1$ defect mode is characterized by a very unusual behavior of the dispersion, which is pronounced in the radiative region and becomes very flat in the guided region,

where the mode propagates with low group velocities [21]. Such unique dispersion characteristics are substantially different as compared with conventional waveguides and PhC fibers, and are peculiar to the photonic confinement achieved in W1 line defects.

VI. Conclusion

One- and two-dimensional SOI PhC waveguides have been successfully fabricated by means of EBL and RIE. Quasi-guided and truly guided modes of the photonic structures have been directly probed by means of angle- and polarization-resolved reflectance and ATR measurements, leading to the determination of photonic bands dispersion both above and below the light line. For the 1-D sample, a linewidth analysis of the guided resonances observed in experimental spectra has been applied according to the Airy–Fano model. Good agreement with theoretical predictions has been obtained and it has been shown that quasi-guided modes with low losses may exist in the radiative region. The propagation characteristics of linear defects embedded in 2-D lattice have also been investigated in details. The resulting dispersion is in very good agreement with full 3-D calculation based on the expansion of the magnetic field on the guided modes. The ATR technique has proven to be a very powerful mean to probe the guided modes of PC slabs.

References

[1] J. D. Joannopoulos, R. D. Meade, and J. N. Winn, *Photonic Crystals Molding the Flow of Light*. Princeton, NJ: Princeton Univ. Press, 1995.

[2] K. Sakoda, *Optical Properties of Photonic Crystals*. New York: Springer-Verlag, 2001.

[3] T. F. Krauss and T. Baba, "Feature section on photonic crystal structures and applications," in *IEEE J. Quantum Electron.*, 2002, vol. 38.

[4] S. G. Johnson and J. D. Joannopoulos, *Photonic Crystals: The Road from Theory to Practice*. Norwell, MA: Kluwer, 2002.

[5] D. Peyrade, Y. Chen, A. Talneau, M. Patrini, M. Galli, L. C. Andreani, E. Silberstein, and P. Lalanne, "Fabrication and optical measurements of silicon on insulator photonic nanostructures," *Microelectron. Eng.*, vol. 61-62, pp. 529–536, 2002.

[6] V. N. Astratov, D. M. Whittaker, I. S. Culshaw, R. M. Stevenson, M. S. Skolnick, T. F. Krauss, and R. M. De La Rue, "Photonic band-structure effects in the reflectivity of periodically patterned waveguides," *Phys. Rev. B*, vol. 60, pp. R16255–R16258, 1999.

[7] V. N. Astratov, I. S. Culshaw, R. M. Stevenson, D. M. Whittaker, M. S. Skolnick, T. F. Krauss, and R. M. De La Rue, "Resonant coupling of near-infrared radiation to photonic band structure waveguides," *J. Lightw. Technol.*, vol. 17, pp. 2050–2057, 1999.

[8] V. Pacradouni, W. J. Mandeville, A. R. Cowan, P. Paddon, J. F. Young, and S. R. Johnson, "Photonic band structure of dielectric membranes periodically textured in two dimensions," *Phys. Rev. B*, vol. 62, pp. 4204–4207, 2000.

[9] L. C. Andreani and M. Agio, "Photonic bands and gap maps in a photonic crystal slab," *IEEE J. Quantum Electron.*, vol. 38, pp. 891–898, 2002.

[10] L. C. Andreani, "Photonic bands and radiation losses in photonic crystal waveguides," *Phys. Status Solidi (b)*, vol. 234, pp. 139–146, 2002.

[11] L. C. Andreani and M. Agio, "Intrinsic diffraction losses in photonic crystal waveguides with line defects," *Appl. Phys. Lett.*, vol. 82, pp. 2011–2013, 2003.

[12] D. M. Whittaker and I. S. Culshaw, "Scattering-matrix treatment of patterned multilayer photonic structures," *Phys. Rev. B*, vol. 60, pp. 2610–2618, 1999.

[13] M. Patrini, M. Galli, F. Marabelli, M. Agio, L. C. Andreani, D. Peyrade, and Y. Chen, "Photonic bands in patterned silicon-on-insulator waveguides," *IEEE J. Quantum Electron.*, vol. 38, pp. 885–890, 2002.

[14] U. Fano, "Effects of configuration interaction on intensities and phase shifts," *Phys. Rev.*, vol. 124, pp. 1866–1878, 1961.

[15] R. F. Kazarinov and C. H. Henry, "Second-order distributed feedback lasers with mode selection provided by first-order radiation losses," *IEEE J. Quantum Electron.*, vol. QE-21, p. 144, 1985.

[16] T. Ochiai and K. Sakoda, "Dispersion relation and optical transmittance of a hexagonal photonic crystal slab," *Phys. Rev. B*, vol. 63, 125107 (7 pp.), 2001.

[17] D. Gerace and L. C. Andreani, "Gap maps and intrinsic diffraction losses in one-dimensional photonic crystal slabs," *Phys. Rev. E*, vol. 69, 056603 (9 pp.), 2004.

[18] M. Galli, M. Agio, L. C. Andreani, M. Belotti, G. Guizzetti, F. Marabelli, M. Patrini, P. Bettotti, L. Dal Negro, Z. Gaburro, L. Pavesi, A. Lui, and P. Bellutti, "Spectroscopy of photonic bands in macroporous silicon photonic crystals," *Phys. Rev. B*, vol. 65, 113111 (4 pp.), 2002.

[19] S. G. Johnson, S. Fan, P. R. Villeneuve, J. D. Joannopoulos, and L. A. Kolodziejski, "Guided modes in photonic crystal slabs," *Phys. Rev. B*, vol. 60, pp. 5751–5758, 1999.

[20] M. Galli, M. Belotti, D. Bajoni, M. Patrini, G. Guizzetti, D. Gerace, M. Agio, L. C. Andreani, and Y. Chen, "Excitation of radiative and evanescent defect modes in linear photonic crystal waveguides," *Phys. Rev. B*, vol. 70, 081307R (4 pp.), 2004.

[21] M. Notomi, K. Yamada, A. Shinya, J. Takahashi, C. Takahashi, and I. Yokohama, "Extremely large group velocity dispersion of line-defects waveguides in photonic crystal slabs," *Phys. Rev. Lett.*, vol. 87, p. 243902(4), 2001.

M. Galli received the Diploma degree in physics and the Ph.D. degree from the University of Pavia, Pavia, Italy, in 1994 and 1999, respectively.

From 1999 to 2000, he held a Postdoctoral position granted by the European Science Foundation (ESF) at the Technical University of Wien. Since 2001, he has held a Postdoctoral position at the Optical Spectroscopy Laboratory, University of Pavia. His main research activities concern strongly correlated electron systems, silicides, and, recently, spectroscopy of photonic crystals.

D. Bajoni was born Italy, in 1976. He received the M.S. degree (the Italian "Laurea") and the Ph.D. degree in physics from the University of Pavia, Pavia, Italy, in 2000 and 2004, respectively.

He currently holds a Postdoctoral position at the Laboratoire de Photonique et de Nanostructures, Marcoussis, France. His main research interests are optical properties of photonic bandgap structures and radiation-matter interactions in low-dimensional nanostructures.

M. Belotti was born in Italy, in 1977. He received the M.S. degree (the Italian "Laurea"). He is currently working towards the Ph.D. degree in physics at the Università degli Studi di Pavia, Pavia, Italy, and also at the Laboratoire de Photonique et de Nanostructures, Marcoussis, France.

His main research interests are nanofabrication and optical properties of photonic bandgap structures.

F. Paleari received the Diploma degree in physics from the University of Pavia, Pavia, Italy, in 2003.

She is now working for a private company.

M. Patrini received the Diploma and Ph.D. degrees in physics from the University of Pavia, Pavia, Italy, in 1992 and 1997, respectively.

From 1998 to 2000, she held a Postdoctoral position granted by Scuola Normale Superiore, Pisa, Italy, and Saint Gobain Recherche, Italy, to perform research on clusters supported in amorphous matrix. Since 2000, she has been with the University of Pavia as a Research Scientist. Currently, she is involved in the experimental activity concerning the optical properties of photonic crystals. Her main research interests are the optical properties of materials investigated by means of optical spectroscopies.

G. Guizzetti received the Degree in physics from the University of Pavia, Pavia, Italy, in 1968.

From 1972 to 1986, he was an Associate Professor at the University of Pavia, from 1979 to 1980, he was a Visiting Scientist at Ecole Polytechnique Federale de Lausanne (EPFL), Lausanne, Switzerland, from 1986 to 2001, he was a Full Professor of Physics of Semiconductors at the University of Pavia. From 1985 to 2000, he was Project Leader of CNR National Projects (MADESS, Solid-State Electronic, MASTA, Silicon-Germanium), ASI Projects, and Network EU. He was Regular Referee of the *Applied Physics Letters*, *Journal on Applied Physics*, *Physics Revision B*, and the *European Physical Journal B*. He has authored more than 150 scientific papers on referred international journals, including international textbooks and handbooks on the optical properties of solids. His recent research activities concerned the study of the optical, electronic and vibrational properties, and the diagnostics, using optical spectroscopy techniques, of the following systems: semiconductors heterostructures (thin films, QWs, SLs, QDs): transition-metal silicides; diamond-like and fullerene, photonic crystals.

D. Gerace was born in Napoli, Italy, in 1977. He received the M.S. degree (the Italian "Laurea") and the Ph.D. degree in physics from the University of Pavia, Pavia, Italy, in 2001 and 2005, respectively.

He currently holds a Postdoctoral position at the University of Pavia. His main research interests are strongly correlated electron systems in low-dimensional semiconductor nanostructures, and theory and modeling of radiation-matter interaction in photonic crystals.

M. Agio was born in Piacenza, Italy, in 1975. He received the Diploma degree (the Italian "Laurea") in 1999, and the Ph.D. degree in physics from the University of Pavia, Pavia, Italy.

He was a Research Scholar at Ames Laboratory, Ames, IA, from September 1999 to December 1999. He currently holds a Postdoctoral position at the ETH, Zurich. His main research interests are theory and modeling of photonic crystal structures.

L. C. Andreani received the Ph.D. degree in physics from Scuola Normale Superiore, Pisa, Italy, in 1989. His dissertation focused on excitons and polaritons in semiconductor nanostructures.

He then was a Postdoctoral Fellow at IRRMA-Ecole Polytechnique Fédérale de Lausanne, Lausanne, Switzerland, working on strongly correlated electron systems. In 1992, he became a Researcher and in 1998 an Associate Professor at the University of Pavia. Since 2000, he has been strongly involved in the physical investigations of photonic crystals, both from the theoretical side and in collaboration with experimentalists in Pavia and in other laboratories. His research interests span several areas in theoretical condensed matter physics, in particular, the optical properties of semiconductors and their heterostructures. His most significant works concern excitons and radiation-matter interaction in quantum wells and in microcavities.

D. Peyrade was born in Toulouse, France, in 1973. He graduated from the Physics Department of INSA and received the M.Sc. degree in physics and microelectronics from the Université Paul-Sabatier, Toulouse, France, in 1997, and the Ph.D. degree from the Groupe d'Etude des Semiconducteurs (Montpellier) and the Laboratoire de Photonique et de Nanostructures, Marcoussis, France.

He is now with CEA LETI, Grenoble, France. His main interests are nanofabrication, optical characterization, and modeling of photonic crystals in GaN and SOI.

Yong Chen received the Ph.D. degree from the University of Montpellier, Montpellier, France, in 1986.

He is a Director of Research at the Centre National de la Recherche Scientifique (CNRS), Laboratoire de Photonique et de Nanostructures, Marcoussis, France. Prior to joining CNRS in 1990, he worked at the Scuola Normale Superiore of Pisa and the University of Beijing between 1987 and 1990. He has published over 160 papers. His current interests are in the development of advanced nanofabrication technologies, as well as prospective applications.